IFEL-Chicane Based Microbuncher at 800nm

Christopher M.S. Sears, Eric Colby, Christopher Barnes

Stanford Linear Accelerator Center, Menlo Park, CA 94025

Abstract. As a first stage to net acceleration in a laser based EM structure RF electron pulses must be microbunched to match the laser wavelength. We report on the design of an undulator and chicane for microbunching at 800nm using an inverse free electron laser (IFEL) interaction. This includes design considerations for the hardware itself, the laser IFEL interaction and bunching performance, and a full 3D particle tracking simulation to study the focusing effects and possible emittance growth due to the fringe fields of the magnets. The talk will close with a discussion of laser-electron beam diagnostics for overlap in the undulator and for diagnosing microbunching performance.

Introduction

The microbunching hardware will work as part of experiments under the E-163 project at SLAC [1]. The hardware consists of two magnet assemblies: the first is an undulator array for modulating the energy of the RF bunch, the second a chicane to bunch the electrons longitudinally. A laser copropagates with the electrons through the undulator to setup an inverse free-electron-laser (IFEL) interaction. A similar scheme has been successfully used by the STELLA collaboration to microbunch at 10.6 μm [2]. The undulator is planar hybrid-Halbach array with a 1.8 cm period and 3 periods. The gap is adjustable to account for possible changes to the beam energy. 60 MeV electrons interact with a 1 ps, 1 mJ laser pulse with a width ~400 μm through the undulator inducing a 0.1 % energy modulation on the bunch. The chicane is three H-magnets, the center one twice the thickness of the outer two, and uses both permanent magnet and coils to steer the beam.

Hardware Design

The most important constraint to the design of the microbunching hardware is the amplitude of the IFEL interaction. If the energy modulation is too small little to no microbunching will occur and net acceleration will be hard to detect. However, in the initial stages of the E-163 experiment acceleration energies will only be a few tens of keV. If the induced energy spread from the IFEL is much greater than this it will again be difficult to detect the acceleration. We therefore set the energy modulation at 0.1% or 60 keV. This can be further tuned by varying the laser intensity (either directly or via the spot size). The strength of the chicane is in turn set by the amplitude of the modulation.

In addition the fields of the undulator and chicane must be designed to eliminate any possible net dipole kick or transverse displacement of the electron bunch. These are quantified by the first and second field integrals:

$$1^{st}(x) = \int_{-\infty}^{x} B_w(x')dx' \quad \text{and} \quad 2^{nd}(x) = \int_{-\infty}^{x}\int_{-\infty}^{x'} B_w(x'')dx''dx' \quad (1)$$

Where B_w is the magnitude of the transverse magnetic field and x is along the direction of propagation of the electrons. Any useful design must have these two integrals equal to zero. The total strength of the chicane can be defined by another field integral proportional to the path length increase of the electrons. This I call the second squared field integral.

$$2^{nd}sq(x) = \int_{-\infty}^{x}\left[\int_{-\infty}^{x'} B_w(x'')dx''\right]^{2}dx' \quad (2)$$

Knowing the momentum modulation induced by the IFEL on the electron bunch we can predict the final density modulation and therefore set the strength of the chicane via this integral.

Further restrictions are placed on the design of the magnetic hardware by the desired focal properties. It is well known that a planar undulator is focusing across the gap and can have a weak defocusing effect transversely due to finite width. To keep fabrication simple, the chicane H-magnets have rectangular faces (non-sector bend magnets) and thus also contribute a small vertical focusing effect. The horizontal defocusing is made negligible by making the poles wide; all are 4 centimeters. The vertical focusing is unavoidable and influences the design toward larger gaps although this also decreases the field strength. A simple particle tracker code is used to monitor the focusing effects of the hardware and explore possible emittance increasing non-linearities. A cold beam (zero initial transverse momentum) is pushed through a three-dimensional field profile dumped from the magnetostatic solver programs used to design the magnets.
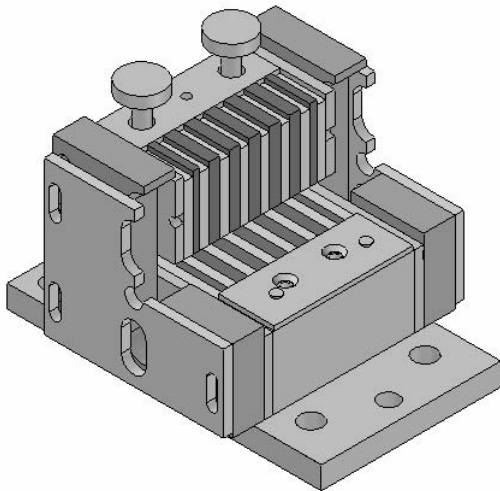
Period	18 mm
Number of Periods	3
Width	40 mm
Gap Height	5-15 mm
End Plate offset	4 mm
Pole height	30 mm
Pole thickness	4 mm
Magnet height	32 mm
Magnet thickness	5 mm
End Plate Aperture	8 mm

Up: Table 1: Undulator dimensions.
Left: Figure 1: CAD drawing of undulator.

The undulator magnet and chicane were designed and simulated in a variety of programs. Pandira, a two-dimensional magnetostatic code was used initially to obtain a rough design. Mafia and Radia (which runs with in Mathematica via Mathlink) were then used to fine tune the design and do tolerance studies. Genesis [4] was used to

study the IFEL interaction and from that we settled upon 3 periods of 1.8 cm length and an on axis field strength of around 0.5 Tesla. With an 800 nm laser with 0.2 mJ of energy per pulse this induces an energy modulation of 0.1% or 60 keV on the 60 MeV electron bunch. This in turn constrains the design of the chicane. Given an overall length of 10 cm (somewhat arbitrary, but constricted by the physical dimensions of the experimental area balanced with practical magnetic fields needed to bunch the beam) the bend angle for the chicane is 60 mrad (or ~3°). The magnets are neodinium-iron-boron (NdFeB) with residual induction B_r = 1.25 T and an energy-product of 37 MG*Oe.
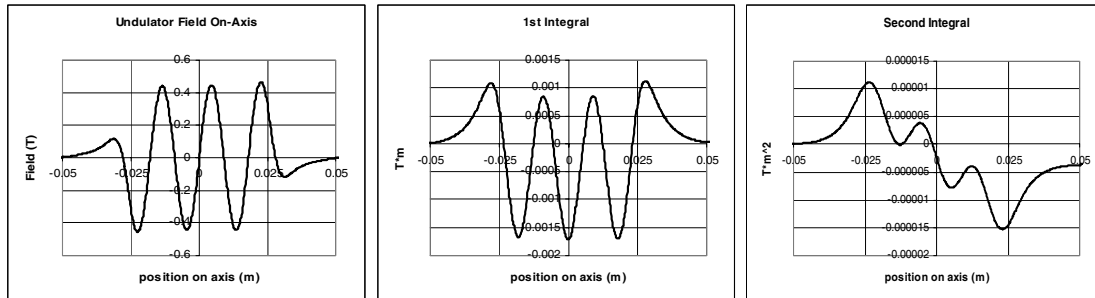
Figure 2: Measured on axis field and field integrals for E-163 undulator. Notice the second integral doesn't quite return to zero by the end of the undulator. This corresponds to a residual 'side-step' of the electrons of 16 microns.

The poles are vanadium permendur and the gap is adjustable, allowing for FEL resonance at 800 nm for beam energies of 55 to 65 MeV. In addition to the 3 main periods there are additional half periods at either end that are necessary to tune the second integral to zero. Also visible in the CAD image on the previous page are the end plates that give a clean truncation of the fields and prevent possible magnetic interference with the chicane. Surrounding the magnets and poles is the stainless steel holding structure, which includes the screws for gap adjustment, and additional screws in the base plate of the device for positioning and fixing within the experimental area. Both the undulator and chicane were fabricated in-house at SLAC.

Simulation also included mechanical tolerance studies to check effects of magnetization direction errors, strength errors, and top/bottom misalignment. Since the hardware is iron dominated, that is the direction of the field is determined primarily by the presence of the iron poles, the possibility of direction errors is negligible. The top & bottom halves also tend to be self-aligning. One place that an error can be introduced, however, is in the positioning of the two endplates relative to the magnet arrays. Shims are used to obtain some correction, however as seen in figure 2, a small misalignment is still present. However, this leads to only a 16 micron side-step, which can easily be corrected for by either the upstream steering, or by steering using the chicane downstream. Particle tracking through the simulated fields give an idea of possible emmittance growth as well as the focal properties of the magnet. The emittance growth in both dimensions is less than 0.1 mm-mradian (compared to 1.25 mm-mrad initial emittance). The vertical focal length is ~6.5 meters, the horizontal defocusing is negligible.
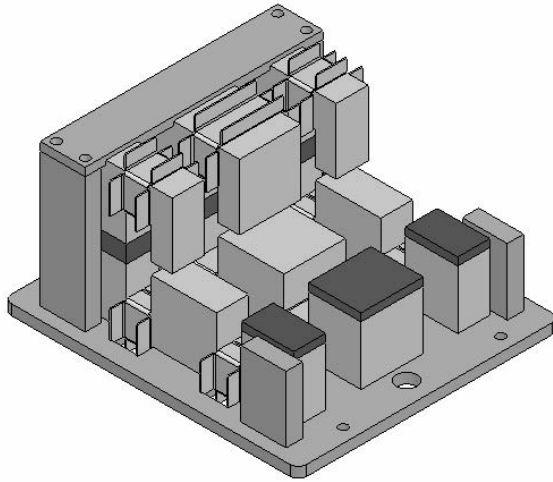
Figure 3: CAD image of chicane. Yellow magnetic iron, red magnets, grey copper. (coils not shown)

The design for the chicane follows similar steps as the undulator, although since it involves no coupling of a laser field simulation was far simpler. After choosing a length for the chicane the angular kick of the H-magnets are found by considering the path lengths of electron trajectories through the chicane. We find the magnitude of the second squared field integral by considering the transformation of the sinusoidal energy variation from the chicane. Notice the chicane path length difference is linear in the energy modulation. Optimal bunching occurs when the slope of the longitudinal phase space diagram goes to infinity around the bunching points. This occurs when

$$2^{nd} sq(x) = \frac{\lambda}{2\pi} \left(\frac{\gamma mc}{e} \right)^2 \left(\frac{\gamma}{\Delta\gamma} \right).$$

In our case the right-hand side equals $5.3*10^{-6}$ $T^2 m^3$ (for 0.1% IFEL modulation). For a chicane with a total length of 10 cm this corresponds to bend angles ~60 mrad and transverse deviation of 2 mm.

As previously stated, the H-magnets are hybrids, with permanent magnets in the back legs and coils in the top spaces. The coils are capable of providing a ±15% variation in the field strength which can cover a ±15% change in the IFEL energy modulation or about ±10% in the mean energy of the bunch. The permanent magnets are again the NdFeB B_r=1.25 T that is used in the undulator. The thicknesses of the H-magnets are 38 mm and 19.5 mm for the inner and outer magnets respectively with a center-to-center separation of 50 mm giving an effective length of the chicane of 10 cm. The support structure for the H-magnets is made of copper to conduct away heat from the coils. The current plan for the hardware placement is to put everything within one large vacuum can, thus heat removal is of key importance to avoid damaging the magnet blocks. Right (Fig. 4) is the field on-axis through the chicane.

Chicane Field On-Axis (no current)
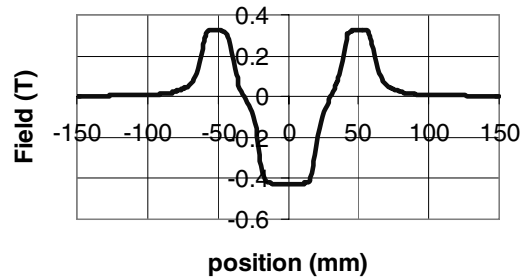
Figure 4: Field on axis through chicane, no current to coils.

The gap for the chicane is fixed at 7 mm, all poles have a width of 40 mm and share a single axis even though the electrons will pass 2 mm off center through the center H-magnet. Particle tracking codes show this will cause no problems. From the particle tracking we infer an estimate for emittance growth through the chicane of 0.05 mm-mrad in the vertical and 0.1 mm-mrad in the horizontal, well below the emittance of the beam itself. The focusing strength of the chicane is 3 meters in the vertical and –50 meters in the horizontal, also negligible compared to the focusing imposed by upstream quads. The H-magnets all rest on a single base plate which uses the same mechanism of precision screws and lock-down screws to adjust the height of the chicane with respect to the electron beam.

Microbunching Performance

Equations for bunching of electron beams were first formulated for non-relativistic beams in klystrons [5]. In klystrons, bunching is from velocity modulation and time-of-flight. Here, the IFEL interaction replaces the velocity modulation in a cavity. Since both processes are linear, however, the same equations apply. The longitudinal density modulation can be written as a cosine expansion with Bessel function coefficients [5].

$$\rho(z) = \rho_0 \left[1 + \sum_{n=1}^{\infty} J_n(n\beta)\cos(k_B z) \right] \qquad (3)$$

Here β describes the degree of bunching with β=1 giving maximal bunching and β>1 overbunched. This equation can be further refined [6,7] to include an initial energy spread by modifying the coefficients to include attenuation terms:

$$\alpha(n) = \exp\left[-\left(\frac{n\sigma_\gamma}{2\eta}\right)^2 \right] \qquad (4)$$

Here, η is the IFEL modulation amplitude, and σ_γ the initial energy spread. Further attenuation terms can be included to account for electron beam divergence and laser wavefront curvature. These, however, tend to be much smaller corrections compared to the initial energy spread term. Figure 5 shows the evolution of the longitudinal distribution for maximum bunching and η/σ_γ=2.5. The simulated performance is degraded compared to the analytical result due to wavefront curvature and residual angular flight exiting the chicane.
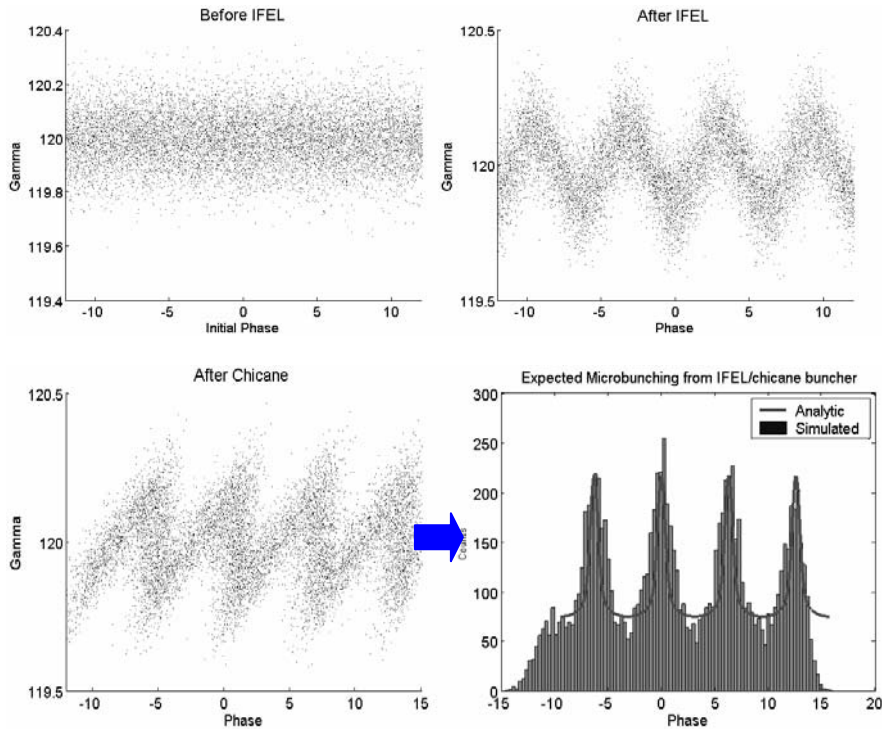
Figure 5: Simulation of microbunching. longitudinal phase space before IFEL (upper left), after (upper right), and after chicane (lower left). Lower right is histogram of longitudinal density, solid curve is analytical result [5].

Diagnostics

In order to successfully microbunch the electron beam overlap between laser and electrons must be achieved. The spatial overlap is obtained by observing the both beams on two yttrium aluminum garnet (YAG) screens placed before and after the undulator. Each screen is inserted into the beam separately and viewed using a series of mirrors by a long distance microscope located outside the vacuum can. The microscope objective is capable of obtaining a 2 millimeter field of view from a half meter distance giving a resolution of approximately 10 microns per pixel on a standard CCD camera. The effective resolution will likely be made worse by camera saturation, beam spot irregularities, and dust on the YAG.

The timing overlap will follow the same procedure described elsewhere for the LEAP experiment [8]. The system obtains a rough (~ 10ns) overlap with a photodiode and then using a streak camera gets the temporal overlap down to ~10 ps. The beam and laser are then scanned over the remaining range to find a signal.

Another diagnostic that would be useful is a means to confirm the microbunching structure after the chicane. Other projects have used coherent transition radiation (CTR) [2,9] to observe microbunched beams. In such schemes the amount of light produced is dependent on the transverse size of the beam relative to gamma times the microbunching wavelength (equation 6).

$$I \propto \exp\left[-\frac{k^2\sigma^2}{\gamma^2} \right] \qquad (6)$$

Unfortunately in the case of the E-163 experiment, this factor is impossibly small; no radiation will be produced. A yet untested idea for getting around this problem is to shape the radiator surface to radiate coherently for a large electron spot. This means the radiator looks like a series of rings, with the spacing equal to gamma times the microbunching wavelength. The transverse term for this device is given in figure 6.
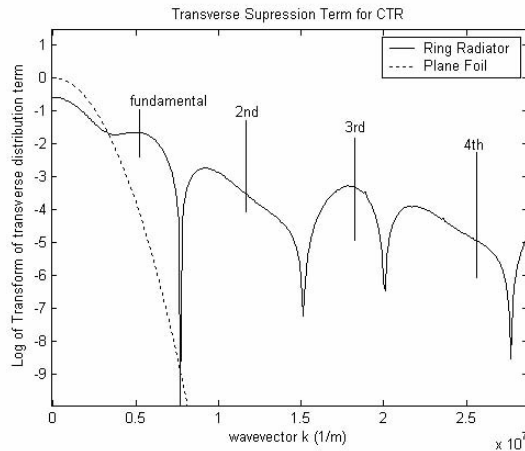
Figure 6: Improved CTR radiator.
Shown in transverse term for
coherent radiation

Conclusion

The development of simple, reliable hardware for microbunching RF electron pulses is a key step to the development of a laser accelerator. The inverse FEL interaction in a planar undulator followed by a chicane offers a simple solution. The hardware described here will soon be placed into experiments under the E-163 project at SLAC. While an emphasis for this design is on minimizing the energy modulation necessary to microbunch, future efforts at laser acceleration may be able to do away with this restriction and obtain tighter bunching from a stronger IFEL interaction. The gradient of the laser accelerator would then provide an upper limit on the induced spread by limiting what size spread can be successfully captured and accelerated.

References

1. See http://www-project.slac.stanford.edu/e163/ for full project description.
2. W.D. Kimura, et. al. Phys. Rev. S.T. Acc. & Beams 4 101301 (2001)
3. C.A. Brau. Free Electron Lasers. Boston: Academic Press, c1990.
4. S. Reiche. Nucl. Instrum. Methods A 429, 243 (1999).
5. P.L. Webster. J. Appl. Phys. 10, 501 (1939).
6. S. Baccaro, F. De martini, & A. Ghigo. Opt. Lett., 7, 174 (1982).
7. A. Luccio, G. Matone, L. Miceli, & G. Giordano. Lasers and Particle Beams. vol. 8, no. 3, 383-398 (1990).
8. Barnes, CD; Colby, ER; Plettner, T. AIP Conference Proceedings; 2002; no.647, p.294-9 Conference: Advanced Accelerator Concepts Tenth Workshop, 22-28 June 2002, Mandalay Beach, CA, USA
9. Tremaine, A, et. al. Nuclear Instruments & Methods in Physics Research, Section A (Accelerators, Spectrometers, Detectors and Associated Equipment); 11 June 1999; vol.429, no.1-3, p.209-129.